Received: 1 March 2024 | Accepted: 7 June 2024

DOI: 10.1111/1751-7915.14511

MICROBIAL BIOTECHNOLOGY Open Access

RESEARCH ARTICLE

Development of a whole-cell biosensor for ethylene oxide and ethylene

Claudia F. Moratti[1] | **Sui Nin Nicholas Yang**[1] | **Colin Scott**[2] | **Nicholas V. Coleman**[3]

[1]School of Life and Environmental Sciences, University of Sydney, Camperdown, New South Wales, Australia

[2]CSIRO Advanced Engineering Biology Future Science Platform, Black Mountain Research & Innovation Park, Canberra, Australian Capital Territory, Australia

[3]School of Natural Sciences and ARC Centre of Excellence in Synthetic Biology, Macquarie University, North Ryde, New South Wales, Australia

Correspondence
Nicholas V. Coleman, School of Natural Sciences and ARC Centre of Excellence in Synthetic Biology, Macquarie University, North Ryde, NSW 2109, Australia.
Email: nicholas.coleman@mq.edu.au

Funding information
Australian Government; Commonwealth Scientific and Industrial Research Organisation

Abstract

Ethylene and ethylene oxide are widely used in the chemical industry, and ethylene is also important for its role in fruit ripening. Better sensing systems would assist risk management of these chemicals. Here, we characterise the ethylene regulatory system in *Mycobacterium* strain NBB4 and use these genetic parts to create a biosensor. The regulatory genes *etnR1* and *etnR2* and cognate promoter P_{etn} were combined with a fluorescent reporter gene (fuGFP) in a *Mycobacterium* shuttle vector to create plasmid pUS301-EtnR12P. Cultures of *M. smegmatis* mc^2-155(pUS301-EtnR12P) gave a fluorescent signal in response to ethylene oxide with a detection limit of 0.2 μM (9 ppb). By combining the epoxide biosensor cells with another culture expressing the ethylene monooxygenase, the system was converted into an ethylene biosensor. The co-culture was capable of detecting ethylene emission from banana fruit. These are the first examples of whole-cell biosensors for epoxides or aliphatic alkenes. This work also resolves long-standing questions concerning the regulation of ethylene catabolism in bacteria.

INTRODUCTION

Biosensors are devices that use biological components to detect or quantify a particular analyte; these may be deployed in a wide range of contexts including industrial facilities, environmental management and healthcare (Bhalla et al., 2016). Biosensors contain two components—a biological sensor and a physical transducer—and are broadly classified based on the nature of each of these components (Banu et al., 2020; Vaidya & Annapure, 2019). The biological components of the sensors include enzymes, proteins, antibodies, nucleic acids, phages or whole cells, while the physical transducers could be optical, electrochemical, thermoelectric, piezoelectric or electrochemical. Transcription factor-based biosensors are a subset of whole-cell biosensors that make use of regulatory proteins and their cognate promoters. In their original contexts, transcription factors modulate gene expression in response to an intracellular or environmental signal, while in biotechnology, they are instead often linked to the expression of a fluorescent protein as the transducer (Tellechea-Luzardo et al., 2023). Transcription factor-based biosensors are particularly valuable in metabolic engineering and can be used to screen or select desirable properties (Mahr & Frunzke, 2016; Rogers et al., 2015). They are cost-effective to produce and can be engineered to have high sensitivity and selectivity (Jeon et al., 2022).

Aerobic bacteria that grow on alkanes or alkenes use monooxygenase (MO) enzymes as the first step in the oxidation of these substrates, yielding epoxides or alcohols, respectively (Shennan, 2006). Bacterial MO's are typically inducible by the initial hydrocarbon

substrate or a downstream metabolite; this is a sensible strategy for the host cell given both the exotic nature of the substrates and the physiological stress of MO expression (Leak et al., 2009). In the alkane-oxidising bacteria, regulatory systems controlling MO expression are well characterised, and many have been developed into biosensors for alkanes or their metabolites (Dietrich et al., 2013; Grant et al., 2014; Jaspers et al., 2001; Kumari et al., 2011; Lehtinen et al., 2017; Li et al., 2013; Minak-Bernero et al., 2004; Reed et al., 2012; Santala et al., 2012; Sevilla et al., 2017; Sticher et al., 1997; Wu et al., 2015; Zhang et al., 2011, 2012); this research field has been recently reviewed (Moratti et al., 2022). In contrast, the regulation of alkene oxidation in bacteria has not been well studied; some regulatory genes (Broberg & Clark, 2010; Coleman et al., 2011; Mattes et al., 2010) and inducers (Dawson et al., 2020; Ensign, 1996; Mattes et al., 2007) have been identified or predicted, but rigorous evidence for specific interactions between inducers, regulatory proteins and promoters has not been presented to date, limiting the development of this biotechnology.

Hydrocarbon biosensors have many potential applications, but to date, the primary focus has been on detection of alkanes (especially octane) as a marker for bioremediation of oil spills (Grant et al., 2014; Jaspers et al., 2001; Kumari et al., 2011; Li et al., 2013; Reed et al., 2012; Sevilla et al., 2015; Sticher et al., 1997; Zhang et al., 2012). Some of these alkane biosensors exploit the *alk* system, first intensively studied in *Pseudomonas putida* GPo1, which consists of the *alkBFGHJKL* structural genes and the *alkST* regulators (Canosa et al., 1999; Panke et al., 1999; Sticher et al., 1997; Van Beilen et al., 2001). The AlkS regulator binds to C6-C10 alkanes, and thus overlaps with the substrate range of its cognate MO AlkB and acts as a direct biosensor for liquid alkanes. In other cases, these binding profiles are divergent; for example, the butane oxidation system of *Thauera butanivorans* involves induction of the BmoR regulator by 1-butanol (Kurth et al., 2008), while the BmoXYBZDC MO preferentially attacks butane (Cooley et al., 2009). Thus, although it controls growth on alkanes, this is an alcohol biosensor rather than an alkane biosensor (Dietrich et al., 2013).

Some Actinobacteria can grow on ethylene via an MO-mediated pathway that proceeds via ethylene oxide (epoxyethane, EtO) as the first intermediate (Coleman et al., 2011; Coleman & Spain, 2003a, 2003b; Hartmans & De Bont, 1992; Mattes et al., 2005, 2010). A subset of these bacteria also grow on the chlorinated derivatives of these compounds (vinyl chloride [VC] and chlorooxirane) and are of special interest for bioremediation. The initial ethylene/VC-oxidising enzyme EtnABCD (a soluble di-iron monooxygenase [SDIMO]) and the epoxide-transforming enzyme EtnE (epoxyalkane-coenzyme M transferase) have been partially characterised (Coleman & Spain, 2003a, 2003b; McCarl et al., 2018), however, the downstream metabolic pathway and the regulation of this pathway are thus-far uncharacterised. The regulatory components of the ethylene oxidation system are of great interest since these may provide the genetic parts for the construction of an ethylene biosensor. Ethylene is not only the most important industrial organic chemical by volume (International Agency for Research on Cancer, 1994) but also the ripening hormone for many fruits and vegetables (Burg & Burg, 1965), furthermore, it is a hazardous compound due to its high flammability (National Center for Biotechnology Information, 2004). Therefore, an ethylene biosensor would be valuable, with multiple possible commercial applications.

Recent preliminary work identified two putative regulatory genes, *etnR1* and *etnR2*, associated with the ethylene oxidation genes in *Mycobacterium* strain NBB4 and showed via gel-shift assay that purified EtnR1 protein bound to a DNA region predicted to contain a promoter (Moratti et al., 2016). Here, we aimed to confirm and extend these initial observations, by showing that EtnR1 and EtnR2 are indeed the regulators of the ethylene oxidation pathway, by localising their cognate promoter and by investigating the inducer range and kinetic properties of the regulatory system. Finally, we aimed to use these genetic components to develop a prototype of a whole-cell ethylene biosensor.

EXPERIMENTAL PROCEDURES

Strains, media, solutions and reagents

Details of strains used in this study are given in Table S1. *E. coli* TOP10 cells (Invitrogen) were used as the primary hosts for plasmid construction and were cultured in Lysogeny Broth (LB) medium (Sambrook et al., 1989). *M. smegmatis* mc^2-155 cells (Snapper et al., 1990) were used as the biosensor chassis; these were cultured in LB for routine purposes or minimal salts medium (MSM) for fluorescence experiments (Coleman et al., 2002). A detailed guide to preparing the MSM medium is provided in Table S2. For mc^2-155 cultures grown in MSM, 10 mM glucose was provided as the carbon and energy source, and 0.05% (v/v) Tween 80 was added to minimise clumping. Both *E. coli* and *M. smegmatis* cultures were grown aerobically at 37°C, with broths shaken at 200 rpm. Kanamycin was added at 50 μg/mL for *E. coli* and 20 μg/mL for *M. smegmatis*. Antibiotics, glucose, Tween80, cumate and the trace metals solution for MSM were all added from filter-sterilised stocks after autoclaving; all these components were made as aqueous stock solutions except cumate which was dissolved in 100% ethanol. Agar was added to media where needed at 15 g/L. All molecular biology enzymes (BsaI-HFv2, T4 DNA ligase, Q5 polymerase) were supplied by NEB. Synthetic DNA fragments and

oligonucleotides were supplied by either IDT or Twist Bioscience. Ethylene (99.5%), ethylene oxide (500 mg/mL in DMSO), ethylene glycol (99.8%), DMSO (99.5%) and cumic acid (98%) were from Sigma–Aldrich.

Plasmid construction

Details of plasmids used in this study are given in Table S1. pUS116 (6.6 kb) (AddGene #84578) is a *Mycobacterium-E. coli* shuttle vector that contains the pUC and pAL5000 origins of replication (*oriE*, *oriM*), kanamycin resistance, and an acetamidase-inducible promoter (Triccas et al., 1998). Plasmid pUS116-etnABCD (11 kb) contains the *etnABCD* MO from *M. chubuense* NBB4 cloned into pUS116; this was made in a previous study (McCarl et al., 2018). pUS301 (5.8 kb) was constructed in this study by amplifying the cumate regulatory system and fuGFP gene from pUS250-fuGFP with primer pair CFM3/CFM4 and cloning the PCR product into XbaI/BamHI-digested pUS116. pUS301-EtnR12P was then made by amplifying the entire pUS301 plasmid (primers CFM202/CFM206, which added BsaI sites to the ends of the amplicon), digesting with BsaI, and ligating via Golden Gate assembly with three BsaI-digested synthetic DNA fragments containing *etnR1* (1860 bp), *etnR2* (751 bp) and P_{etn} (290 bp). pUS301-EtnR1P and pUS301-EtnR2P were constructed via amplification of different sub-sections of pUS301-EtnR12P (primers CFM261/CFM262 and CFM179/CFM260, respectively), then circularisation of the amplicons by Golden Gate reaction with BsaI and ligase. pUS301-EtnR12P promoter truncation plasmids were constructed by amplifying the plasmid to exclude P_{etn} (primers CFM206/CFM294), then ligating via Golden Gate assembly with synthetic DNA fragments containing truncated P_{etn} sequences (P_{etn}-20: 270 bp, P_{etn}-60: 230 bp, P_{etn}-80: 210 bp, P_{etn}-100: 190 bp). Details of PCR primers used in this study are provided in Table S3. Plasmid features and sequences of pUS301, pUS301-EtnR12P and pUS116-etnABCD are provided in GenBank format in Sections S2 and S3.

Biosensor growth, induction and fluorescence assays

The following method was used for the initial identification of inducers, characterising the response to different EtO concentrations, testing the requirement for etnR1 and etnR2, and testing truncated versions of the P_{etn} promoter. Cells of *M. smegmatis* were transformed with the biosensor plasmid (pUS301-EtnR12P or pUS301-EtnR1P or pUS301-EtnR2Pvia electroporation (2.5 kV, 800 Ω, 25 μF, 2 mm cuvette gap)). After 4 days incubation, a loopful of growth (several colonies) was transferred into 5 mL LB + Km + Tween, grown to saturation (48 h), then cells were collected by centrifugation for (15,000 *g*, 10 min). The cells were resuspended in 5 mL of MSM + Km + Tween+glucose broth, and then a subsample of the cell suspension was inoculated into 50 mL of the same medium to give an initial OD_{600} of 0.02. Cultures were grown to OD_{600} = 0.25–0.50 (approx. 18–20 h), then 3 mL of culture was added to a sterile 26 mL glass vial. Cumate was added to 100 μM, then vials were crimp-sealed with Teflon-faced butyl rubber stoppers. Ethylene was added as a neat gas to give 10% v/v in the headspace, whereas ethylene oxide and ethylene glycol were added as 100 μM stock solutions in DMSO to give 1 μM in the liquid phase (3 μL stock solution per 3 mL of culture). Controls lacked either cumate or the test inducers; in the latter case, DMSO only was added. The vials were incubated horizontally with shaking to ensure good gas exchange. A sampling of cells was done 16–20 h post-induction via extracting 200 μL of culture with a syringe and transferring the sample to a 96-well plate (polystyrene, flat-bottom, black-edged, Greiner #655090). Fluorescence was measured in a plate reader (ClarioStar Plus, BMG Labtech) at 470 nm excitation and 515 nm emission, in both cases with a bandwidth of 20 nm, with the gain set to 1000. The culture turbidity (OD_{600}) was measured at the same time, and the RFU was calculated as fluorescence/OD_{600}. For the EtO concentration curve, samples were collected 10 h post-induction with cumate and inducer.

For the time course assay, the above method was modified by scaling the system up to 24 mL cultures in 120 mL crimp-sealed bottles, and by sampling at multiple time points over a 29-h incubation. For testing the effect of pre-induction of the regulators, the original protocol above was modified by adding cumate at the point of transfer of the starter culture into the 50 mL broth, and by adding EtO 16–20 h later, after the culture had reached an OD_{600} = 0.25–0.3. For the co-culture assay, the original protocol was modified by inclusion of a second culture of mc^2-155, carrying plasmid pUS116-etnABCD; these cells were prepared similarly to the mc^2-155(pUS301-EtnR12P) cells (i.e. freshly transformed with plasmid, pre-grown in a 5 mL broth, then transferred to a 50 mL broth), except that they were induced with acetamide (1%) instead of cumate at the point of transfer into the 50 mL broth. In this experiment, the pre-induction method was used for the mc^2-155(pUS301-EtnR12P) culture, so it was also induced with cumate at the point of transfer into the larger broth. After the respective inducer additions, both cultures were grown until OD600 = 0.25–0.50 (~18 h), then the cultures were mixed at different volumetric ratios (50:50, 90:10, 10:90) in the 26 mL test vials to give a total culture volume of 3 mL. After crimp-sealing, ethylene was added to the headspace (2% v/v), the cultures were incubated 16 h with shaking, then fluorescence and OD_{600} were measured in the plate reader as described

above, and RFU was calculated. GraphPad Prism was used to fit the Hill equation to the data set and calculate the Hill coefficient and K_m values (Sigmoidal, 4PL, X is concentration, nonlinear regression).

$$\text{Hill equation: } V = \frac{V_{\max}[S]^n}{(K_m)^n + [S]^n},$$

where V is the response, S is the substrate, K_m is the substrate concentration that gives half the maximum response, and n is the Hill coefficient.

Detection of ethylene emission from fruit

Cultures of mc^2-155(pUS301-EtnR12P) and mc^2-155(pUS116-etnABCD) were separately grown in 50 mL MSM + Km + Tween+glucose broths, induced with cumate or acetamide, respectively, and harvested at mid-exponential phase, as described above. The cells were centrifuged and resuspended to OD_{600} = 5 in the same medium, then mixed at a ratio of 2:1 (biosensor cells:epoxidating cells) in 3 mL total volume and added into 16 mL glass vials with no cap. Fresh produce items, either carrot or banana, were sliced into 3-mm-thick discs which were then further chopped in half, and then 10 g of material was added to separate 100 mL Schott bottles. The vials containing the biosensor co-culture were suspended with string inside each bottle, then the bottles were tightly capped, and incubated at room temperature for 3 days with shaking (150 rpm). The fluorescence of the cell suspensions was then visualised qualitatively under long-wave UV light (405 nm emission maximum) using a hand-held torch.

RESULTS

Bioinformatic analysis of the *etnR1* and *etnR2* regulators and P_{etn} promoter

The predicted ethylene catabolism genes are located on a 144 kb plasmid in *Mycobacterium* NBB4 (Genbank CP003055). Inspection of this locus (Figure 1) reveals two possible regulatory gene candidates, *etnR1* (Mycch_5972) and *etnR2* (Mycch_5971). Several lines of bioinformatic evidence support a role for both these genes in the regulation of the ethylene MO and other alkene catabolic genes, as described below.

The *etnR1* and *etnR2* genes are embedded within a larger gene cluster containing the *etnABCD* MO and several other genes either known or suspected to play a role in alkene metabolism (Mattes et al., 2010); these are all in the same orientation, suggesting a common promoter, that is, they form an operon. It is typical for transcription activators to have a low level of constitutive expression that is upregulated in the presence of the correct inducer (Stekel & Jenkins, 2008); thus we postulate that EtnR1 and EtnR2 are initially expressed at low levels from an as-yet-unidentified constitutive promoter immediately upstream and then are upregulated via a positive feedback loop upon activation of the operon in the presence of the hydrocarbon inducer. There is precedent for this in the AlkS system of *P. oleovorans* (Canosa et al., 2000).

BLAST analysis of EtnR1 and EtnR2 provides evidence that these comprise a two-component sensing system, with EtnR2 as the sensor, and EtnR1 as the DNA-binding protein. EtnR1 is a member of the CdaR superfamily of regulatory proteins (COG3835), with homology to CdaR over the region from amino acids 250–554 (E-value = 1.8e^{-21}). The CdaR regulator itself is an activator of sugar-diacid catabolism in *E. coli* (Monterrubio et al., 2000). A helix-turn-helix (HTH) domain, common to DNA-binding proteins, is present at the C-terminus of EtnR1 (amino acids 501–561), with homology to the HTH domain of the *Bacillus subtilis* PucR regulator; this regulator controls purine catabolism in *B. subtilis* (Beier et al., 2002). EtnR1 also contains a GAF domain (amino acids 135–285) similar to those found in transcriptional activators such as FhlA and NifA; GAF domains are common in sensory proteins (Ho et al., 2000).

EtnR2 contains just one conserved domain that spans most of the protein (amino acids 21–174, E value = 3.42e−46); this is a methanogen/methylotroph DcmR sensory (MEDS) domain. MEDS domains are involved in the sensing of small hydrocarbons

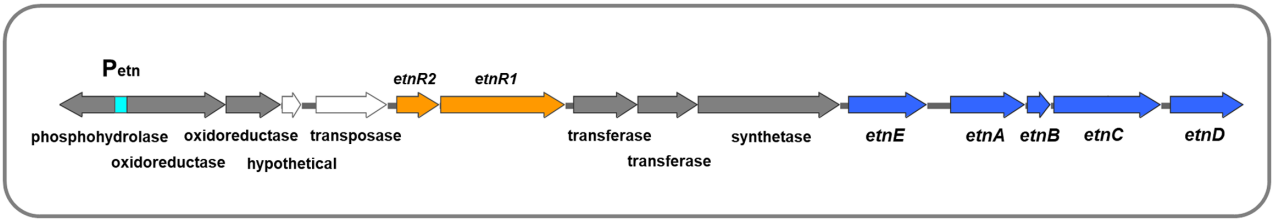

FIGURE 1 Ethylene metabolic genes and regulators in strain NBB4. Metabolic genes of known function are in blue, predicted metabolic genes are in grey, and predicted regulatory genes are in orange. The predicted promoter region (P_{etn}) is in cyan. The region shown is 16.5 kb in size and represents only part of the complete ethylene catabolism and coenzyme M biosynthesis locus, which is approx. 40 kb. The genes shown are Mycch_5966–Mycch_5980, nucleotides 20621–37183 of plasmid pMYCCH.02 of strain NBB4.

and their derivatives and were first identified in methanogens and methylotrophs (Anantharaman & Aravind, 2005). EtnR2 has 24% amino acid identity and 34% amino acid similarity to the archetypal protein in this family, the DcmR dichloromethane sensor of Methylobacterium sp, strain DM4 (La & Leisinger, 1991). EtnR2 lacks the N-terminal HTH domain seen in DcmR; this is unsurprising since DcmR acts as a single stand-alone regulator (transcriptional repressor) while EtnR2 most likely acts together with EtnR1. We hypothesise that ethylene or a metabolite derived from ethylene binds to EtnR2, which transfers this signal to EtnR1, which then binds to the P_{etn} promoter region, leading to the activation of expression of the ethylene catabolic genes.

Homologues of *etnR1* and *etnR2* are present within the predicted ethylene catabolic gene clusters of all other known ethylene/vinyl chloride-oxidising Actinobacteria (Figure 2), and these homologues are highly conserved in sequence and location relative to the genes in strain NBB4 (Genbank NC_018023). However, more distant homologues also occur in Actinobacteria with no known capability for hydrocarbon oxidation; these can be subdivided into one group which co-occur with genes similar to those involved in alkene oxidation and/or CoM biosynthesis (these may be bacteria with yet-to-be-demonstrated alkene oxidation capacities), and another group which do not colocalise with catabolic genes. The EtnR1/R2 regulatory system appears to be a specialised subset of a broader group of regulators with thus far unknown functions, which are common in the Actinobacteria.

Based on inspection of the NBB4 genome sequence, the promoter for the ethylene catabolic genes was predicted to occur in a 167 bp non-coding region that is 4 kb upstream of the regulatory genes (Figure 1). This region is positioned between two divergently oriented gene clusters, with the predicted coenzyme M (CoM) biosynthesis genes on one side, and the ethylene catabolic genes on the other side. Note that coenzyme M is a key cofactor required for epoxide metabolism by the EtnE enzyme in the alkene

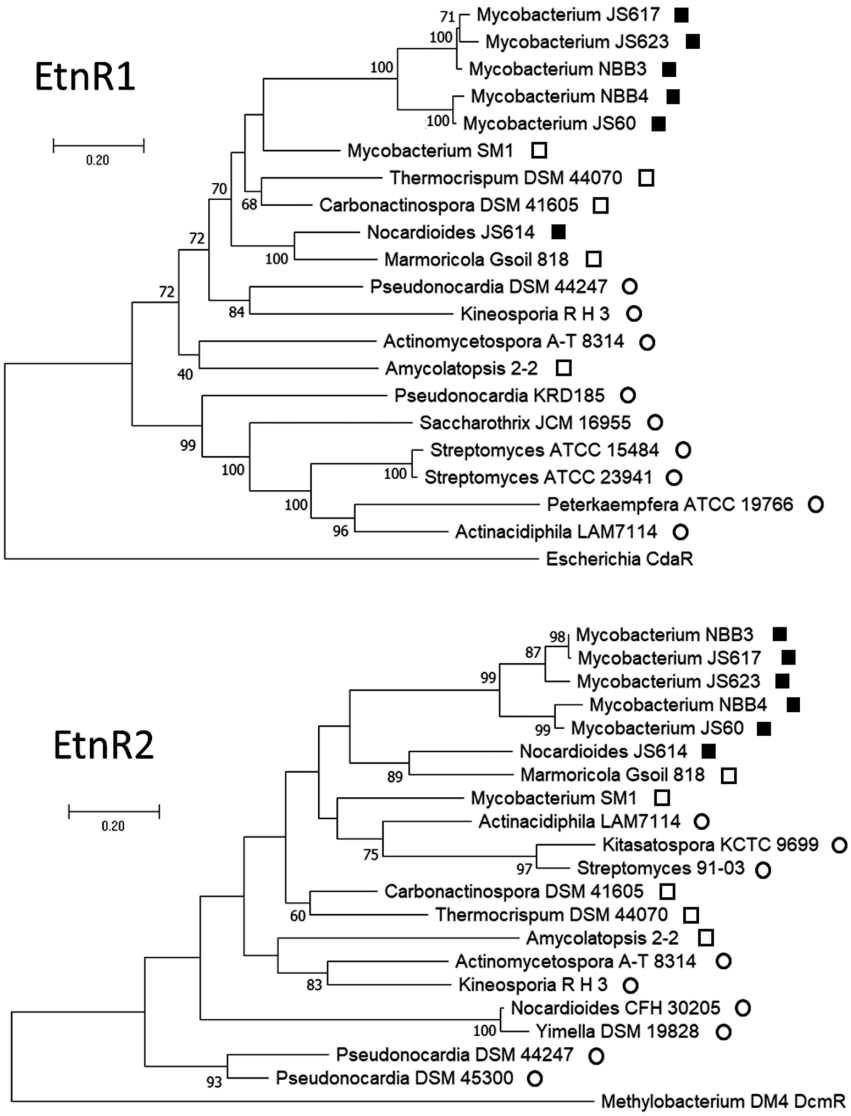

FIGURE 2 Phylogeny of EtnR1 and EtnR2 homologues. EtnR1 or EtnR2 homologues were detected by BLASTp, and representative sequences with 40%–99% identity to the NBB4 proteins were selected for analysis, along with one representative outgroup (CdaR or DcmR). Alignments were generated in MEGA using the MUSCLE algorithm, then trimmed (573 amino acids or 194 amino acids for EtnR1 and EtnR2, respectively). Trees were generated in MEGA11 by maximum likelihood method with 100 replicates. Symbols are as follows; ■, known alkene utilizers; □, alkene catabolism genes near regulator; ○, other types of genes near regulator. Bootstrap values of >50% are shown at nodes.

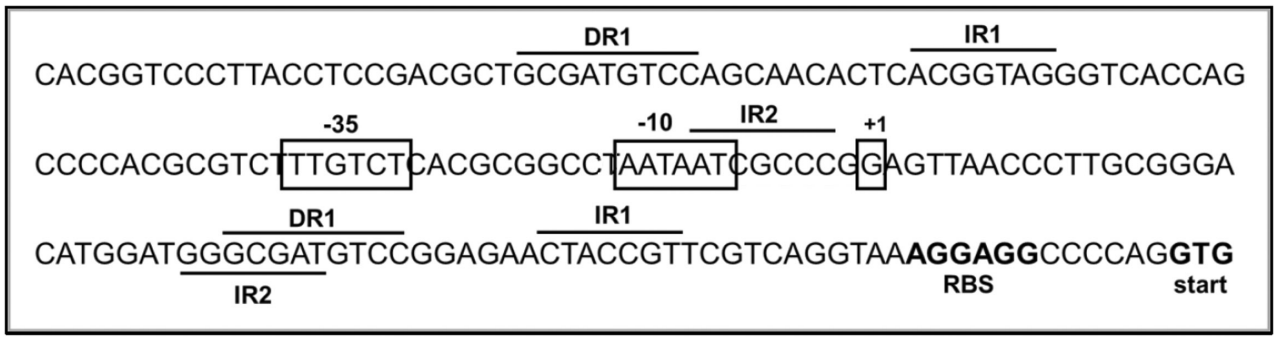

FIGURE 3 DNA sequence and features of predicted promoter region P_{etn}. Predicted -35 and -10 sequences and transcription start (+1) are boxed. Predicted -24 and -12 sequences have dotted underlines or overlines. Inverted repeats (IR1, IR2) and direct repeats (DR1) have solid underlines or overlines. The predicted RBS and start codon for the oxidoreductase gene MYCCH_RS29030 are shown in bold.

catabolic pathway, thus it is logical for the CoM biosynthetic gene clusters to be co-ordinately regulated with the alkene catabolic genes; in aerobic bacteria, the only known function of CoM to date is in alkene catabolism (Partovi et al., 2018). We therefore predict that this non-coding region contains two divergently oriented promoters controlled by the same regulators (i.e. EtnR1/EtnR2). Here we focus our attention just on one component of this region, that is, the promoter driving the ethylene catabolic genes, which we have named P_{etn}.

The predicted P_{etn} promoter (Figure 3) contains putative −35 and −10 sequences (TTGTCT, AATAAT) that are similar to the consensus for σ70 promoters in mycobacteria (TTGACR, TATRMT), and although the spacing of these elements is only 9 bp, this shorter spacing is not uncommon in mycobacteria (Newton-Foot & Gey van Pittius, 2013). The putative P_{etn} promoter region contains several direct and inverted repeat sequences; these are typical binding sites for transcription factors (Newton-Foot & Gey van Pittius, 2013). Sequences similar to the binding sites of EtnR1 homologues such as PucR (WWWCNTTGGTTAA; Beier et al., 2002) or FhlA (CATTTCGTACGAAATG; Leonhartsberger et al., 2000) could not be detected.

Design and construction of biosensor

Mycobacterium smegmatis mc^2-155 was previously shown to be a good expression host for the ethylene MO EtnABCD (McCarl et al., 2018) and thus we reasoned that mc^2-155 would also be appropriate for functional expression of the EtnR1 and EtnR2 regulators. We first constructed a *Mycobacterium/E. coli* shuttle vector, pUS301, which was then used as the backbone for biosensor construction. The annotated sequence of pUS301 is provided in the Appendix S1; this vector contains the pUC origin for replication in *E. coli*, the pAL5000 origin for replication in *Mycobacterium*, a kanamycin resistance gene functional in both genera and a cumate-inducible promoter for expression of cloned genes (Kaczmarczyk et al., 2013). The latter was created by fusing the CymR repressor binding sites (cumate operators; CuO) on each side of the strong P_C promoter from the class 1 integron (Jové et al., 2010).

The prototype biosensor was constructed via Golden Gate assembly of three synthetic DNA fragments (*etnR1*, *etnR2*, P_{etn}) into pUS301, such that *etnR1* and *etnR2*, were co-expressed from the cumate-inducible promoter (Figure 4). Both *etnR1* and *etnR2* were modified from the wild type by removing internal restriction sites via single base changes and by reducing the overall GC content to enable gene synthesis. Both restriction site removal and changes to GC content were done while preserving the amino acid sequence using a manual codon harmonisation strategy, that is, choices of codons in the modified sequence were matched as closely as possible to the relative frequency of the codon in the wild-type gene at that position. The 5′ ends of both regulatory genes were fused to the same synthetic strong ribosome-binding site (AAGGAG), with a 6-bp spacer region before the start codons.

To minimise transcriptional read-through of the cumate-inducible promoter into the P_{etn} promoter and its reporter gene, the strong bidirectional transcription terminator BBa_B1001 from the iGEM Parts Kit was added between *etnR2* and P_{etn}. As a reporter gene to measure transcription, the gene for free-use green fluorescent protein (fuGFP; BBa_K3814004) was positioned immediately downstream of P_{etn}, with 112-bp spacing between the predicted transcription and translation start points. The fuGFP gene was used with the strong RBS BBa_B0034 (Elowitz & Leibler, 2000) separated from the start codon by a 7 bp spacer.

Identification of inducers of the EtnR1-EtnR2-P_{etn} system

Cultures of mc^2-155(pUS301-EtnR12P) were treated with cumate to induce the regulator genes and

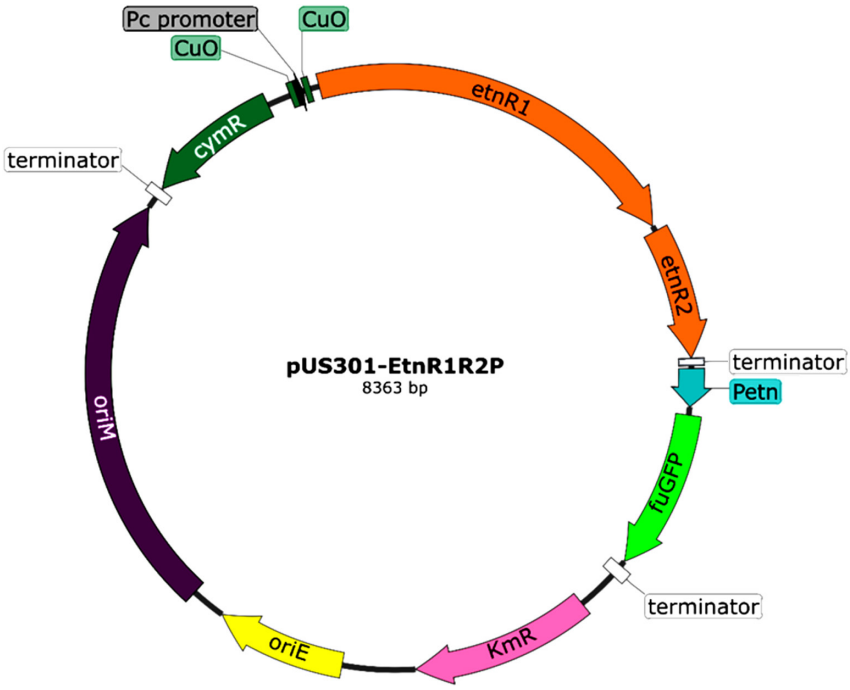

FIGURE 4 Schematic map of biosensor plasmid pUS301-EtnR12P. Key features include Km^R (pink), oriE (yellow), pAL5000 oriM (purple), CymR (dark green). EtnR1 and EtnR2 (orange) and P_{etn} (turquoise). Map was constructed with SnapGene software.

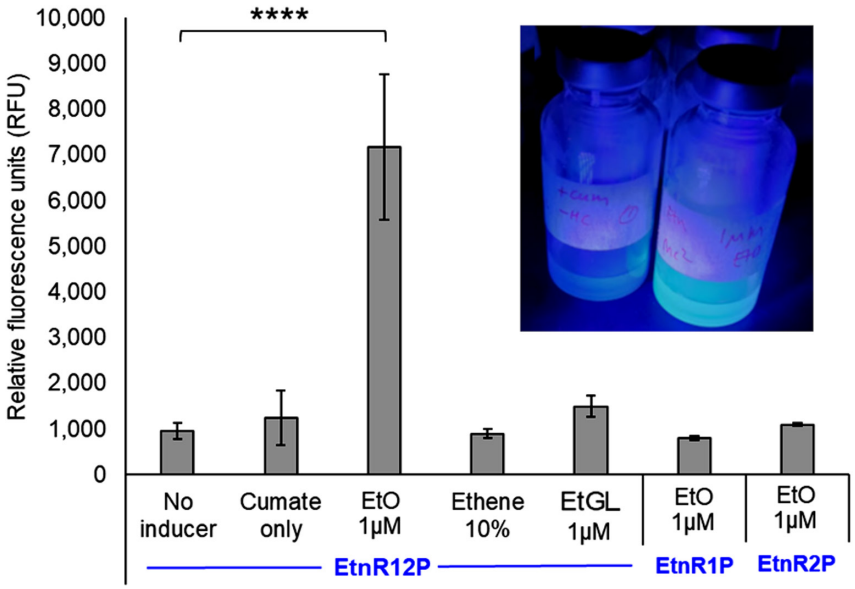

FIGURE 5 Testing inducers of the EtnR1–EtnR2-P_{etn} regulatory system. Liquid inducers (EtO, EtGL) were added as solutions in DMSO, while gases (ethylene) were added neatly to the headspace. RFU values were derived by dividing the raw fluorescence readings by the density (OD_{600}) of the cultures. Data were collected 16 h after inducer addition. Data show the mean of three biological replicates, and error bars show the standard deviation. Statistical analysis was carried out using one-way ANOVA and Tukey post-hoc multiple comparisons analysis, with $p < 0.05$ judged as 'significant'. *$p \leq 0.05$, **$p \leq 0.01$, ***$p \leq 0.001$, ****$p \leq 0.0001$. The inset panel shows the appearance of cultures with and without EtO (1 µM) added, under long-wave UV illumination.

various test compounds (alkenes, epoxides, alcohols) as possible inducers of the EtnR1-EtnR2-P_{etn} system (Figure 5). Cultures induced with cumate only gave the same low fluorescence as the solvent control (DMSO) ($p > 0.05$), providing confidence that any increase in fluorescence would be due to P_{etn} being activated, and not read-through from the cumate-inducible promoter. A strong response was seen after ethylene oxide addition (EtO, 1 µM), with an average fluorescence 8.5-fold greater than the solvent control ($p < 0.05$). (Weak induction (1.8-fold) was seen with ethylene glycol (EtGL, 1 µM) but this was not statistically significant ($p = 0.9518$ vs. uninduced)). Ethylene (10% v/v in headspace) did not give significant

fluorescence ($p > 0.9999$ compared to uninduced sample). Biosensor plasmid variants containing only *etnR1* or *etnR2* (pUS301-EtnR1P, pUS301-EtnR2P) produced no significant fluorescence after exposure to EtO, confirming that both genes are necessary for the system to function; this experiment also confirms that EtnR1 is an activator rather than a repressor since if the latter were true, P_{etn} should have switched on when *etnR1* was removed, regardless of the presence of the epoxide inducer.

Characterisation of biosensor sensitivity and response range with EtO

The responses of mc^2-155(pUS301-EtnR12P) cultures were tested with a range of EtO concentrations (Figure 6A). The minimum concentration giving a significant fluorescent response (i.e. the measured detection limit of the biosensor) was 0.2 μM EtO (= 9 ppb), and the response reached a maximum of around 50 μM (= 2200 ppb). It should be noted that these are nominal concentrations, that is, assuming that all EtO is dissolved in the liquid phase; this is a reasonable approximation given the low Henry's constant for ethylene oxide ($H^{cp} = 5.8 \times 10^{-2}$) (Conway et al., 1983). Calculation of the predicted amount of EtO in the liquid phase using Henry's constant gives a similar number (8.17 ppb; see Section S1). The transfer function of the biosensor relating the inducer concentration (input) to the fluorescent signal (output) was modelled using the Hill equation, which is often applied to transcription factor–promoter interactions during the regulation of gene expression (Bhaskaran & Nair, 2015; Bottani & Veitia, 2017). The resulting sigmoidal curve when plotted on a logarithmic *x*-axis had a good fit ($R^2 = 0.9486$) and allowed the derivation of key performance parameters (Figure 6B).

Time course of biosensor induction and effect of pre-induction of regulators

A time course assay was done to assess the induction profile of the biosensor with EtO (Figure 7), using cumate only (negative control), co-induction (cumate and EtO added simultaneously) and pre-induction (cumate added 16 h before EtO); the latter test aimed to determine if biosensor response could be accelerated by having the regulator proteins present in the cells before EtO was added. Pre-induction decreased the lag time before RFU began to increase by 1 h and gave a faster initial rate of increase in RFU (252 vs. 192 RFU/h; Figure 10B,C). Co-induction gave an initial linear increase in RFU over the first 18 h ($r^2 = 0.9959$), while for pre-induction, the initial linear increase in RFU was only for 6.5 h ($r^2 = 0.9946$), then the rate slowed to 115 RFU/h between 6.5 and 22 h ($R^2 = 0.985$). At 15 h post-induction, the RFU of the co-induced culture caught up with the pre-induced culture, and after this point, the cultures behaved similarly, reaching a peak RFU at 23 h, then declining. EtO induction did not dramatically impact the growth of cultures (Figure S1), although pre-induction led to a slowing of growth after 12 h relative to co-induction. Overall, the pre-induction method was confirmed to give a more rapid biosensor response.

Localization of P_{etn} promoter sequence

To identify the minimum necessary promoter region, four variants of the 167 bp P_{etn} sequence with different 5′ truncations were assayed for activity (Figure 8). Removal of the first 20 bp of the sequence had no significant impact on biosensor response ($p = 0.8381$). A 60 bp deletion including one copy each of the DR1

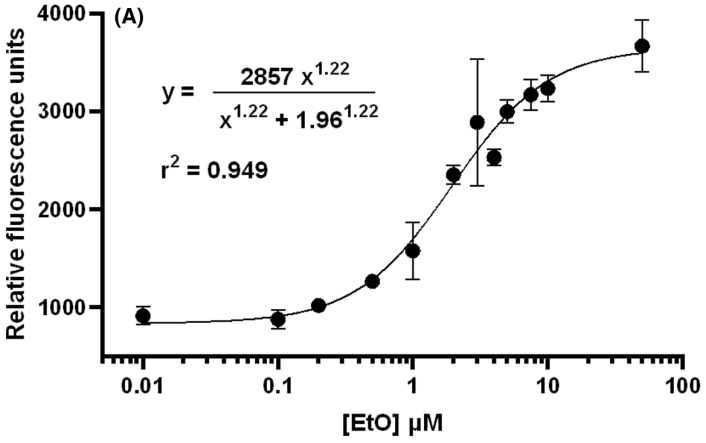

(B)

Performance parameter	Value
Linear range of detection	0.5-10 μM
Sensitivity (n) (Hill coefficient)	1.22
Dynamic range (fold increase)	4.2
K_m (μM)	1.96
R_{lim} (RFU)	3668
Response time to half of maximum (h)	12

FIGURE 6 Epoxide biosensor response to EtO and performance parameters. Panel (A) Plot of biosensor response at different EtO concentrations. RFU values were measured 10 h after simultaneous induction with cumate and EtO. Data points are the mean of four biological replicates, and error bars show the standard deviation. The data have been fitted with a sigmoidal function via the equation shown on the graph. Panel (B) Summary of performance parameters of biosensor with EtO.

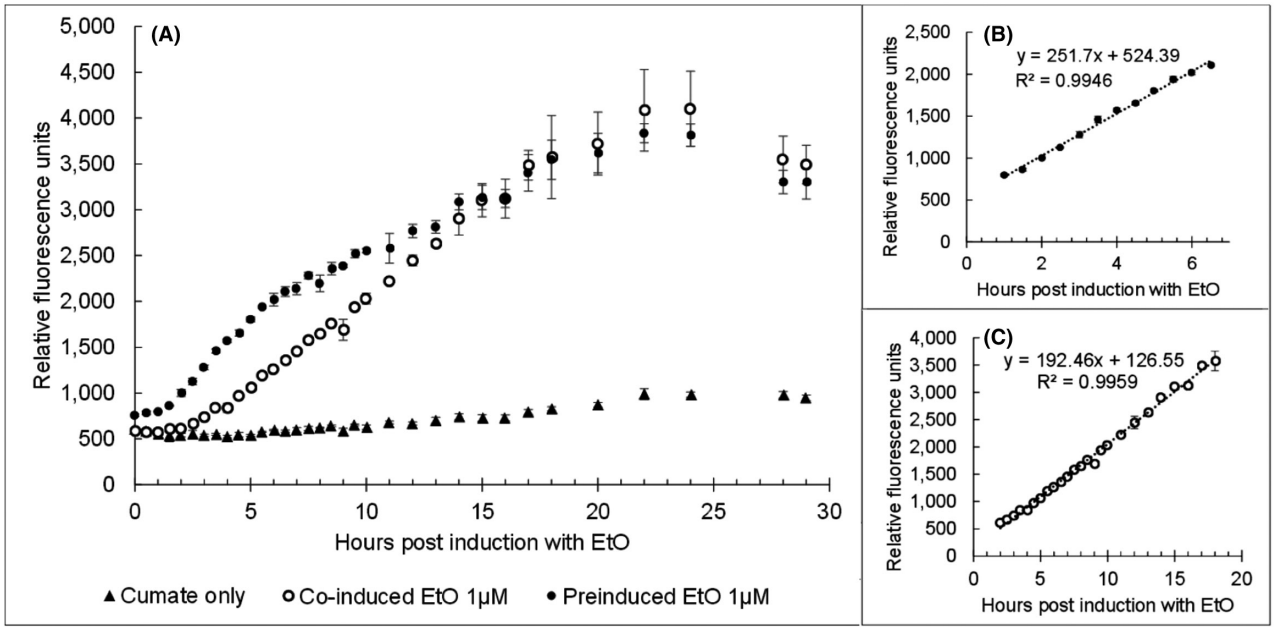

FIGURE 7 Time course of induction of EtO biosensor. Panel (A) Complete time course data of all sample sets. Panel (B) Linear fit through data from pre-induced data set between 1 and 7 h post-induction with 1 μM EtO. Panel (C) Linear fit through data from co-induced data set between 1 and 16 h post-induction with 1 μM EtO. Data are the means of three biological replicates, and error bars show the standard deviation.

FIGURE 8 Localisation of P_{etn} promoter elements via 5′ sequence truncations. Fluorescence data were collected 21 h after induction with 1 μM EtO. Negative controls were induced with cumate only or cumate + DMSO. Data are means of four biological replicates, and error bars show the standard deviation. Statistical analysis was performed by two-way ANOVA, and *p*-values reported in the text are from Tukey post-hoc multiple comparisons analysis with $p < 0.05$ judged as 'significant'. *$p \leq 0.05$, **$p \leq 0.01$, ***$p \leq 0.001$, ****$p \leq 0.0001$.

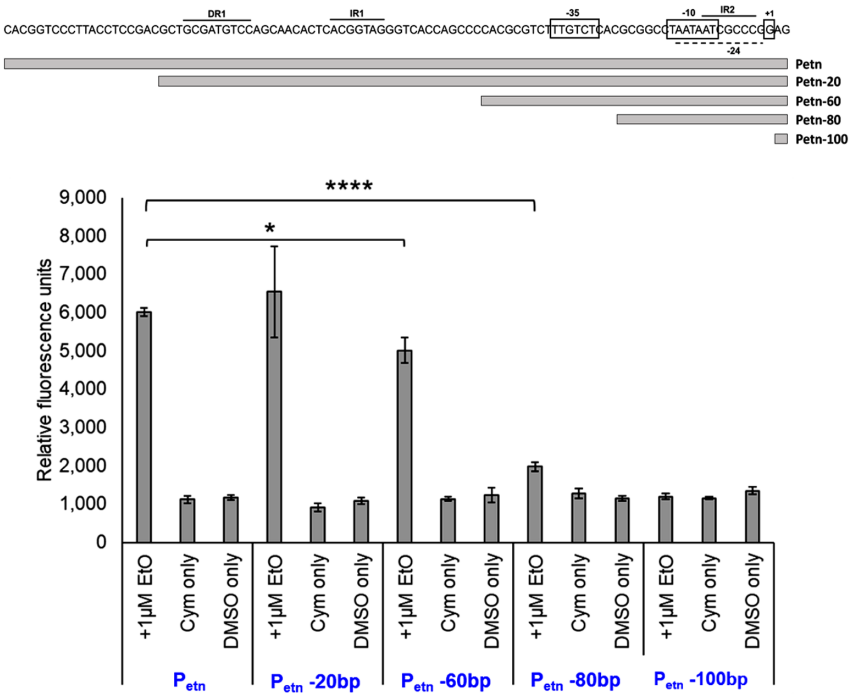

and IR1 repeat elements gave a 20% decrease in RFU ($p = 0.0377$). The 80 bp deletion removed the putative −35 site and resulted in an 80% decrease in RFU; the signal from this construct was not significantly different from the 100 bp deletion construct after EtO induction ($p = 0.2619$) or the negative controls ($p = 0.2040$ no truncation uninduced, $p = 0.1397$ no truncation induced with cumate alone). The 100 bp deletion removed the putative −10 site and led to a complete loss of biosensor activity. Taken together, these results suggest that the P_{etn} promoter is of the σ^{70} type, that the −35 and −10 sequences identified here are the key sites for facilitating RNA polymerase binding and that the DR1 and/or IR1 sequences may be involved in the binding of EtnR1 to the promoter region.

Adding ethylene MO expands the biosensor range to include alkenes

Since alkenes can be converted into epoxides via the action of MO enzymes, we hypothesized that the addition of an MO activity into our biosensor system would enable it to detect alkenes in addition to epoxides. Proof-of-principle for this approach was obtained via a co-culture method, via combining mc^2-155 cells containing pUS301-EtnR12P with mc^2-155 cells containing pUS116-etnABCD; the latter plasmid contains the ethylene MO of *Mycobacterium* NBB4 under the control of an acetamide-inducible promoter (McCarl et al., 2018). Different initial ratios of the two cultures (50:50, 90:10, 10:90) were tested. A strong fluorescent response (equal or better than with ethylene oxide) was seen in the 90:10 and 50:50 mixtures of biosensor:MO cultures after exposure to ethylene ($p < 0.0001$), while the 10:90 mixture was less effective, and the signal from this mixture was not statistically significant ($p > 0.05$) (Figure 9). No significant fluorescence was seen in a 50:50 co-culture lacking ethylene, but interestingly, the biosensor culture alone with ethylene added did give a higher fluorescence in this experiment than the negative control with no biosensor cells (although at $p > 0.05$); this indicates that the mc^2-155 host may have low levels of endogenous alkene MO activity, consistent with earlier work (Furuya et al., 2013). The results confirm that the initial epoxide biosensor can be converted into an alkene biosensor by adding an MO enzyme to the system and that a relatively small amount of MO activity is sufficient to give a strong biosensor response to ethylene.

The co-culture biosensor can detect ethylene emission from fruit

As a test of the 'real world' functionality of the co-culture biosensor, an experiment was devised to determine whether the system could differentiate between two functionally different kinds of fresh produce, that is, one which does not emit ethylene (carrots), and one which emits ethylene (bananas) (Figure 10A). The co-culture biosensor was capable of distinguishing between these, and in the presence of banana, sufficient green fluorescence was obtained to be visible to the eye (Figure 10B). While the fluorescent signal from the banana emissions was much weaker than the fluorescence from biosensor cultures exposed to pure ethylene oxide (see inset in Figure 5), this experiment provides proof of principle that the co-culture biosensor has sufficient sensitivity to detect ethylene in a real-world context and is sufficiently selective such that other volatile emissions from non-ethylene producing items (e.g. carrots) will not interfere.

DISCUSSION

Ethylene-utilising bacteria were first reported nearly 50 years ago (de Bont, 1976), but subsequent progress in understanding their genetics, biochemistry and metabolism has been slow. Notably, most of the steps in the ethylene catabolic pathway and the associated CoM biosynthetic pathway are still unknown. Here, we have made an important advance by pinpointing the inducer and by characterising the regulatory genes and promoter. Epoxides have been previously predicted to

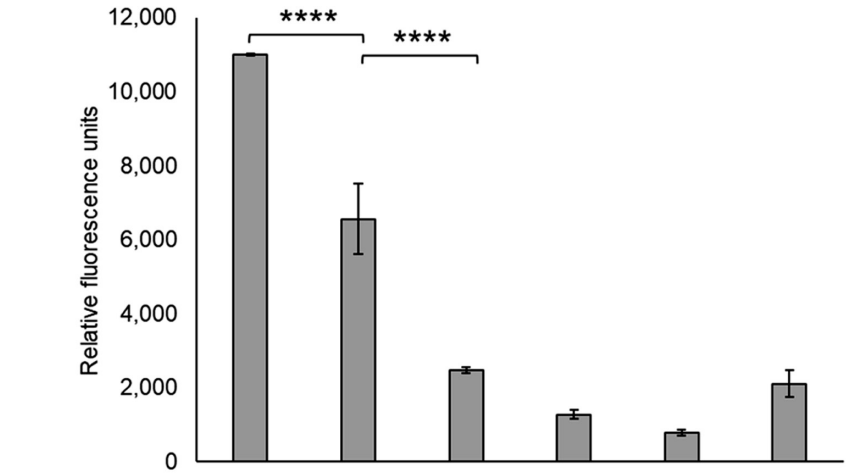

FIGURE 9 Ethylene detection by co-culture of EtO biosensor with MO-expressing cells. Cells of mc^2-155(pUS116-etnABCD) were induced with 1% acetamide, while cells of mc^2-155(pUS301-EtnR12P) were induced with 100 μM cumate. RFU was calculated 21 h after ethylene addition. Data are the mean of three biological replicates. Error bars show the standard deviation. Statistical analysis was performed using one-way ANOVA, and *p*-values from Tukey post-hoc multiple comparisons analysis are presented with $p < 0.05$ judged as 'significant'. *$p \leq 0.05$, **$p \leq 0.01$, ***$p \leq 0.001$ and ****$p \leq 0.0001$.

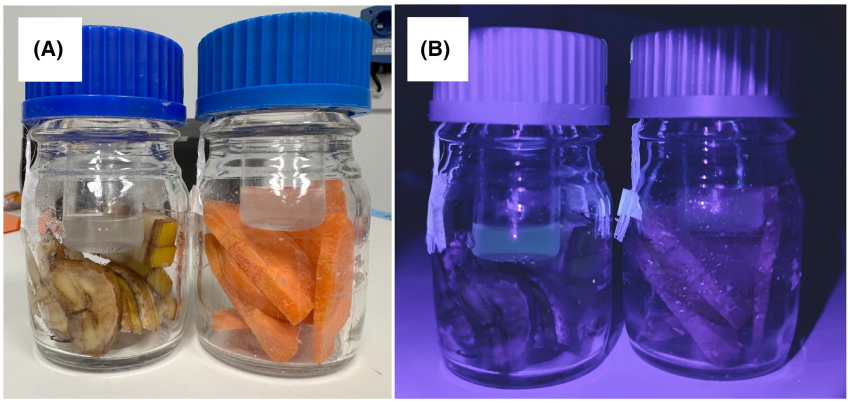

FIGURE 10 Detection of ethylene emission from banana by co-culture biosensor. Panel (A) Visualisation after 3 days incubation under regular white light illumination. Panel (B) Visualisation after 3 days incubation under long-wave UV light illumination.

be the inducers of alkene catabolic systems (Dawson et al., 2020; Ensign, 1996; Mattes et al., 2007), but our work here is the first to identify and characterise the DNAs and proteins involved. Due to the high homology of the NBB4 regulators to those in other ethylene and VC-oxidising *Mycobacterium* isolates, we believe that epoxide-mediated induction is common to all these bacteria.

To the best of our knowledge, the EtnR1–EtnR2 pair is the first example of a bacterial sensing system that responds to an epoxide. This is unusual due to the high reactivity, toxicity and instability of expoides (National Center for Biotechnology Information, 2023). It is unlikely that a further-downstream metabolite is the true inducer, since the host strain mc^2-155 lacks all of the ethylene catabolic and CoM biosynthetic enzymes EtO hydrolyses spontaneously to yield EtGL, but this was a very poor inducer. The control of the ethylene catabolic system resembles that of the butane oxidation system of *T. butanivora* (Dietrich et al., 2013), where the first metabolite (1-butanol) is the inducer; we hypothesise that it is easier for bacteria to evolve sensors for functionalised molecules like alcohols and epoxides compared to the unreactive hydrocarbons that are the primary substrates of these pathways. A potential issue for our biosensor and similar whole-cell biosensors is whether global regulatory systems such as catabolite repression (Moreno & Rojo, 2024) may impact their function. Although the ethylene regulatory genes have been removed from their normal host context, it is possible that common catabolite repression systems exist in both *M.chubuense* and *M.smegmatis* which might impact biosensor function, depending on the media used for experiments.

Promoter truncation assays supported the bioinformatic analysis, indicating that the ethylene catabolic genes are controlled by a σ^{70} type promoter, with −35 and −10 sites, although with non-standard spacing. Although the −35 motif is not universal in mycobacterial promoters (Newton-Foot & Gey van Pittius, 2013), we found that removal of the putative −35 site from the P_{etn} sequence gave an 80% drop in signal, suggesting it is important in this case. The truncation of the sequence upstream of the −35 site caused some reduction in biosensor activity, but this effect was not dramatic. This was expected to have a larger impact on activity since bioinformatic analyses and of the results from deletion of *etnR1* indicate that EtnR1 is an activator, binding upstream of the core σ^{70} promoter (Busby & Ebright, 1994; Langdon & Hochschild, 1999). Further studies to characterise inducer–protein, protein–protein and protein–promoter binding are needed to understand the EtnR1–EtnR2-P_{etn} control system.

Performance parameters for this biosensor were derived from the Hill transformation of the data set, which showed a good fit ($R^2 = 0.9486$). The sensitivity (i.e. Hill coefficient) of pUS301-EtnR12P with EtO (1.22) is comparable to that of P_{BMO} (0.78–2.54 with various inducers) (Dietrich et al., 2013) and to several other common systems induced by small molecules (AraC = 1.3, CdaR = 1.0) (Rogers et al., 2015) but is lower than for BTEX biosensors such as pGLTUR (1.2–3.8) (Willardson et al., 1998). The maximum fluorescence levels and linear range were comparable to that of P_{BMO}. Further work is needed to refine the data obtained here, moving the system into an easier host strain or an in vitro system would enable this and would facilitate future prototyping work.

Co-culture with a strain expressing ethene MO was used here as a novel way to convert the epoxide sensor into an ethylene sensor. Despite the complexities of this experiment, the co-culture produced a higher fluorescent response than the epoxide-sensing single culture. This could be due to continuous production of EtO in the co-culture system, leading to a more sustained biosensor response. Alternatively, continuous production of smaller amounts of epoxide may minimise aqueous hydrolysis or toxic effects. The highest signal in the co-culture system was produced by a 90:10 initial mixture of biosensor:MO cells, indicating that the sensing/output components were the limiting factor rather than the MO activity. While the co-culture here provided proof-of-principle for an

ethylene biosensor, future iterations are required to refine the system, for example, assembly of the MO and regulatory genes in a single plasmid.

EtO is a potent biocide, routinely used for sterilisation of medical equipment (Russell, 1990). If the biosensor were to be deployed in sterilisation contexts, it may need to remain functional in the presence of very high epoxide levels (e.g. 300 mg/L; Biocidal Products Directive, 2020); orders of magnitude higher than the detection threshold of the biosensor determined in this study. Further work is needed to determine at what point EtO toxicity to the chassis bacteria would impact the function of the system. The development of cell-free transcription/translation systems (TXTL) also offers a solution to toxicity issues. The ethylene sensor is not as confounded by analyte toxicity since ethylene itself is less toxic, and only small amounts are needed to trigger the biosensor.

Sensors for EtO are a necessity in workplaces that use this toxic substance since the odour threshold (260 ppm) is much higher than the allowable exposure limits. Our whole-cell EtO biosensor is more sensitive than existing commercially available sensors based on chemical reactions; these have detection ranges of 0–10 ppm, with a resolution of 0.1 ppm (https://evikon.eu/), while our sensor has a detection range of 9–2200 ppb. Although more sensitive EtO sensors do exist in the research literature which can detect parts-per-trillion EtO, these depend on expensive large equipment, that is, an infrared laser direct absorption spectrometer (Yacovitch et al., 2022). Importantly, our EtO sensor can easily detect levels corresponding to recommended workplace exposure limits (OSHA: 1 ppm over 8 h, 5 ppm in 15 min; NIOSH: 0.1 ppm per day, 5 ppm in 10 min) (New Jersey Department of Health, 2016). A limitation of our prototype biosensor is its slow response (several hours); this lags far behind the state of the art, where response times in seconds are possible (Alexandrov & Vickers, 2023) Another drawback is the need for live engineered bacteria of a non-standard host type, which raises regulatory issues. Adapting these parts into a cell-free system may provide solutions to both of these problems.

The ethylene-responsive variant of our biosensor would have applications in the bulk chemical industry (e.g. monitoring workplace exposure and detection of gas leaks) but also would have applications in agriculture and in the fresh produce supply chain. Ethylene management is critical to the control of fruit ripening, whether this relates to endogenous production of the gas by the fruit itself, exposure of the produce to exogenous ethylene or the use of chemical regulators that mimic ethylene and/or inhibit the plant ethylene receptors (Hu et al., 2019; Janssen et al., 2014). Despite these efforts, an inability to effectively monitor fruit ripeness throughout the production chain is a major contributing factor to over 1.3 billion tonnes of food waste generated globally every year, a loss with an equivalent retail value of over USD$1 trillion that contributes ~8% of the global greenhouse gas emissions (FAO, 2014, 2015; Gustavsson et al., 2011; United Nations Environment Programme, 2021). Here, we have provided proof-of-principle that our co-culture biosensor can detect ethylene emissions from bananas. Further development of this biosensor will contribute greatly to solving the intertwined problems of ripening management and minimising food waste.

AUTHOR CONTRIBUTIONS

Claudia F. Moratti: Conceptualization; methodology; formal analysis; investigation; writing – original draft. **Sui Nin Nicholas Yang:** Investigation; writing – original draft. **Colin Scott:** Conceptualization; methodology; formal analysis; supervision; writing – review and editing. **Nicholas V. Coleman:** Conceptualization; methodology; formal analysis; supervision; writing – review and editing.

ACKNOWLEDGEMENTS

CM was supported during her PhD candidature by a Research Training Program scholarship from the Australian Government and by a top-up scholarship and operating costs budget from a CSIRO Synthetic Biology Future Science Platform PhD award. We acknowledge the University of Sydney 2016 iGEM team 'FRESH' (Amanda Chen, Sing-Young Chen, Sholto Douglas, Liam Ferguson, Wunna Kyaw, Claudia Moratti, Orion Tong, Alma Wu) for their contributions to preliminary work on this project. Open access publishing facilitated by Macquarie University, as part of the Wiley - Macquarie University agreement via the Council of Australian University Librarians.

FUNDING INFORMATION

CM was supported by a Research Training Program scholarship from the Australian Government and by a CSIRO Synthetic Biology Future Science Platform PhD award.

CONFLICT OF INTEREST STATEMENT

The authors declare no conflicts of interest in the current work. This manuscript was accepted as a pre-print in bioRxiv on 21 Feb, 2024 (https://doi.org/10.1101/2024.02.19.581074).

DATA AVAILABILITY STATEMENT

All relevant data have been made available either in the main manuscript or in the Appendix S1.

ORCID

Colin Scott https://orcid.org/0000-0001-6110-6982
Nicholas V. Coleman https://orcid.org/0000-0002-3594-1754

REFERENCES

Alexandrov, K. & Vickers, C.E. (2023) In vivo protein-based biosensors: seeing metabolism in real time. *Trends in Biotechnology*, 41, 19–26.

Anantharaman, V. & Aravind, L. (2005) MEDS and PocR are novel domains with a predicted role in sensing simple hydrocarbon derivatives in prokaryotic signal transduction systems. *Bioinformatics*, 21, 2805–2811.

Banu, N.D., Jerca, F.A. & Jerca, V.V. (2020) Biosensors. In: *Food, medical, and environmental applications of polysaccharides*. Amsterdam, Oxford, Cambridge, MA: Elsevier, pp. 381–400.

Beier, L., Nygaard, P., Jarmer, H. & Saxild, H.H. (2002) Transcription analysis of the *Bacillus subtilis* PucR regulon and identification of a *cis*-acting sequence required for PucR-regulated expression of genes involved in purine catabolism. *Journal of Bacteriology*, 184, 3232–3241.

Bhalla, N., Jolly, P., Formisano, N. & Estrela, P. (2016) Introduction to biosensors. *Essays in Biochemistry*, 60, 1–8.

Bhaskaran, S. & Nair, A.S. (2015) Hill equation in modelling transcriptional regulation. In: *Systems and synthetic biology*. Dordrecht: Springer, pp. 77–92.

Biocidal Products Directive. (2020) Ethylene oxide, Document IIIA Section 5.

Bottani, S. & Veitia, R.A. (2017) Hill function-based models of transcriptional switches: impact of specific, nonspecific, functional and nonfunctional binding. *Biological Reviews*, 92, 953–963.

Broberg, C.A. & Clark, D.D. (2010) Shotgun proteomics of *xanthobacter autotrophicus* Py2 reveals proteins specific to growth on propylene. *Archives of Microbiology*, 192, 945–957.

Burg, S.P. & Burg, E.A. (1965) Ethylene action and the ripening of fruits. *Science*, 148, 1190–1196.

Busby, S. & Ebright, R.H. (1994) Promoter structure, promoter recognition, and transcription activation in prokaryotes. *Cell*, 79, 743–746.

Canosa, I., Sánchez-Romero, J.M., Yuste, L. & Rojo, F. (2000) A positive feedback mechanism controls expression of AlkS, the transcriptional regulator of the *pseudomonas oleovorans* alkane degradation pathway. *Molecular Microbiology*, 35, 791–799.

Canosa, I., Yuste, L. & Rojo, F. (1999) Role of the alternative sigma factor σ(s) in expression of the *alkS* regulator of the *pseudomonas oleovorans* alkane degradation pathway. *Journal of Bacteriology*, 181, 1748–1754.

Coleman, N.V., Mattes, T.E., Gossett, J.M. & Spain, J.C. (2002) Biodegradation of *cis*-dichloroethene as the sole carbon source by a β-proteobacterium. *Applied and Environmental Microbiology*, 68, 2726–2730.

Coleman, N.V. & Spain, J.C. (2003a) Distribution of the coenzyme M pathway of epoxide metabolism among ethene- and vinyl chloride-degrading *mycobacterium* strains. *Applied and Environmental Microbiology*, 69, 6041–6046.

Coleman, N.V. & Spain, J.C. (2003b) Epoxyalkane:coenzyme M transferase in the ethene and vinyl chloride biodegradation pathways of *mycobacterium* strain JS60. *Journal of Bacteriology*, 185, 5536–5545.

Coleman, N.V., Yau, S., Wilson, N.L., Nolan, L.M., Migocki, M.D., Ly, M. et al. (2011) Untangling the multiple monooxygenases of *mycobacterium chubuense* strain NBB4, a versatile hydrocarbon degrader. *Environmental Microbiology Reports*, 3, 297–307.

Conway, R.A., Waggy, G.T., Speigel, M.H. & Bergiund, R.L. (1983) Environmental fate and effects of ethylene oxide. *Environmental Science & Technology*, 17, 107–112.

Cooley, R.B., Dubbels, B.L., Sayavedra-Soto, L.A., Bottomley, P.J. & Arp, D.J. (2009) Kinetic characterization of the soluble butane monooxygenase from *Thauera butanivorans*, formerly "*pseudomonas butanovora*". *Microbiology*, 155, 2086–2096.

Dawson, R.A., Larke-Mejía, N.L., Crombie, A.T., Ul Haque, M.F. & Murrell, J.C. (2020) Isoprene oxidation by the gram-negative model bacterium *Variovorax* sp. WS11. *Microorganisms*, 8, 349.

de Bont, J.A.M. (1976) Microbial metabolism of ethylene. *Antonie Van Leeuwenhoek*, 42, 59–71.

Dietrich, J.A., Shis, D.L., Alikhani, A. & Keasling, J.D. (2013) Transcription factor-based screens and synthetic selections for microbial small-molecule biosynthesis. *ACS Synthetic Biology*, 2, 47–58.

Elowitz, M.B. & Leibler, S. (2000) A synthetic oscillatory network of transcriptional regulators. *Nature*, 403, 335–338.

Ensign, S.A. (1996) Aliphatic and chlorinated alkenes and epoxides as inducers of alkene monooxygenase and epoxidase activities in *xanthobacter* strain Py2. *Applied and Environmental Microbiology*, 62, 61–66.

FAO. (2014) *Food wastage footprint: Full-cost accounting*. Rome: Food and Agriculture Organisation of the United Nations. http://library.unccd.int/Details/books/1384

FAO. (2015) Global Initiative on Food Loss and Waste Reduction. https://www.fao.org/save-food/resources/keyfindings/infographics/fruit/en/

Furuya, T., Hayashi, M. & Kino, K. (2013) Reconstitution of active mycobacterial binuclear iron monooxygenase complex in *Escherichia coli*. *Applied and Environmental Microbiology*, 79, 6033–6039.

Grant, C., Deszcz, D., Wei, Y.-C., Martínez-Torres, R.J., Morris, P., Folliard, T. et al. (2014) Identification and use of an alkane transporter plug-in for applications in biocatalysis and whole-cell biosensing of alkanes. *Scientific Reports*, 4, 5844.

Gustavsson, J., Cederberg, C. & Sonesson, U. (2011) *Global food losses and food waste. In save food congress*. Dusseldorf: SIK – The Swedish Institute for Food and Biotechnology.

Hartmans, S. & De Bont, J.A.M. (1992) Aerobic vinyl chloride metabolism in *Mycobacterium aurum* L1. *Applied and Environmental Microbiology*, 58, 1220–1226.

Ho, Y.S.J., Burden, L.M. & Hurley, J.H. (2000) Structure of the GAF domain, a ubiquitous signaling motif and a new class of cyclic GMP receptor. *The EMBO Journal*, 19, 5288–5299.

Hu, B., Sun, D.W., Pu, H. & Wei, Q. (2019) Recent advances in detecting and regulating ethylene concentrations for shelf-life extension and maturity control of fruit: a review. *Trends in Food Science and Technology*, 91, 66–82.

International Agency for Research on Cancer. (1994) Ethylene. In: *IARC monographs on the evaluation of carcinogenic risks to humans: some industrial chemicals*. Lyon: World Health Organisation.

Janssen, S., Schmitt, K., Blanke, M., Bauersfeld, M.L., Wöllenstein, J. & Lang, W. (2014) Ethylene detection in fruit supply chains. *Philosophical Transactions. Series A, Mathematical, Physical, and Engineering Sciences*, 372, 20130311.

Jaspers, M.C.M., Meier, C., Zehnder, J.B., Harms, H. & Van der Meer, J.R. (2001) Measuring mass transfer processes of octane with the help of an *alkS-alkB*::*gfp*-tagged *Escherichia coli*. *Environmental Microbiology*, 3, 512–524.

Jeon, Y., Lee, Y., Kim, K., Jang, G. & Yoon, Y. (2022) Transcription factor-based biosensors for detecting pathogens. *Biosensors-Basel*, 12, 470.

Jové, T., Da Re, S., Denis, F., Mazel, D. & Ploy, M.C. (2010) Inverse correlation between promoter strength and excision activity in class 1 integrons. *PLoS Genetics*, 6, e1000793.

Kaczmarczyk, A., Vorholt, J.A. & Francez-Charlot, A. (2013) Cumate-inducible gene expression system for sphingomonads and other Alphaproteobacteria. *Applied and Environmental Microbiology*, 79, 6795–6802.

Kumari, R., Tecon, R., Beggah, S., Rutler, R., Arey, J.S. & van der Meer, J.R. (2011) Development of bioreporter assays for the detection of bioavailability of long-chain alkanes based on

the marine bacterium *Alcanivorax borkumensis* strain SK2. *Environmental Microbiology*, 13, 2808–2819.

Kurth, E.G., Doughty, D.M., Bottomley, P.J., Arp, D.J. & Sayavedra-Soto, L.A. (2008) Involvement of BmoR and BmoG in n-alkane metabolism in '*pseudomonas butanovora*'. *Microbiology*, 154, 139–147.

La, S.D. & Leisinger, T. (1991) Identification of *dcmR*, the regulatory gene governing expression of dichloromethane dehalogenase in *Methylobacterium* sp. strain DM4. *Journal of Bacteriology*, 173, 6714–6721.

Langdon, R.C. & Hochschild, A. (1999) A genetic method for dissecting the mechanism of transcriptional activator synergy by identical activators. *Proceedings of the National Academy of Sciences of the United States of America*, 96, 12673–12678.

Leak, D.J., Sheldon, R.A., Woodley, J.M. & Adlercreutz, P. (2009) Biocatalysts for selective introduction of oxygen. *Biocatalysis and Biotransformation*, 27, 1–26.

Lehtinen, T., Santala, V. & Santala, S. (2017) Twin-layer biosensor for real-time monitoring of alkane metabolism. *FEMS Microbiology Letters*, 364, 1–7.

Leonhartsberger, S., Ehrenreich, A. & Böck, A. (2000) Analysis of the domain structure and the DNA binding site of the transcriptional activator FhlA. *European Journal of Biochemistry*, 267, 3672–3684.

Li, C., Zhang, D., Song, Y., Jiang, B., Li, G. & Huang, W.E. (2013) Whole cell bioreporter for the estimation of oil contamination. *Environmental Engineering and Management Journal*, 12, 1353–1358.

Mahr, R. & Frunzke, J. (2016) Transcription factor-based biosensors in biotechnology: current state and future prospects. *Applied Microbiology and Biotechnology*, 100, 79–90.

Mattes, T.E., Alexander, A.K. & Coleman, N.V. (2010) Aerobic biodegradation of the chloroethenes: pathways, enzymes, ecology, and evolution. *FEMS Microbiology Reviews*, 34, 445–475.

Mattes, T.E., Coleman, N.V., Chuang, A.S., Rogers, A.J., Spain, J.C. & Gossett, J.M. (2007) Mechanism controlling the extended lag period associated with vinyl chloride starvation in *Nocardioides* sp. strain JS614. *Archives of Microbiology*, 187, 217–226.

Mattes, T.E., Coleman, N.V., Spain, J.C. & Gossett, J.M. (2005) Physiological and molecular genetic analyses of vinyl chloride and ethene biodegradation in *Nocardioides* sp. strain JS614. *Archives of Microbiology*, 183, 95–106.

McCarl, V., Somerville, M.V., Ly, M.A., Henry, R., Liew, E.F., Wilson, N.L. et al. (2018) Heterologous expression of *mycobacterium* alkene monooxygenases in gram-positive and gram-negative bacterial hosts. *Applied and Environmental Microbiology*, 84, e00397.

Minak-Bernero, V., Bare, R.E., Haith, C.E. & Grossman, M.J. (2004) Detection of alkanes, alcohols, and aldehydes using bioluminescence. *Biotechnology and Bioengineering*, 87, 170–177.

Monterrubio, R., Baldoma, L., Obradors, N., Aguilar, J. & Badia, J. (2000) A common regulator for the operons encoding the enzymes involved in D-galactarate, D-glucarate, and D-glycerate utilization in *Escherichia coli*. *Journal of Bacteriology*, 182, 2672–2674.

Moratti, C., Chen, A., Chen, S.-Y., Douglas, S., Ferguson, L., Kyaw, W. et al. (2016) Fruit Ripeness Ethylene Sensor (Hopefully). https://2016.igem.org/Team:Sydney_Australia

Moratti, C.F., Scott, C. & Coleman, N.V. (2022) Synthetic biology approaches to hydrocarbon biosensors: a review. *Frontiers in Bioengineering and Biotechnology*, 9, 804234.

Moreno, R. & Rojo, F. (2024) What are the signals that control catabolite repression in *pseudomonas*? *Microbial Biotechnology*, 17, e14407.

National Center for Biotechnology Information. (2004) Ethylene. PubChem. https://pubchem.ncbi.nlm.nih.gov/compound/Ethylene

National Center for Biotechnology Information. (2023) *Ethylene Oxide*. Bethesda, MD: PubChem. https://pubchem.ncbi.nlm.nih.gov/compound/Ethylene-Oxide

New Jersey Department of Health. (2016) Hazardous Substance Fact Sheet: Ethylene oxide. https://nj.gov/health/eoh/rtkweb/documents/fs/0882.pdf

Newton-Foot, M. & Gey van Pittius, N.C. (2013) The complex architecture of mycobacterial promoters. *Tuberculosis*, 93, 60–74.

Panke, S., Meyer, A., Huber, C.M., Witholt, B. & Wubbolts, M.G. (1999) An alkane-responsive expression system for the production of fine chemicals. *Applied and Environmental Microbiology*, 65, 2324–2332.

Partovi, S.E., Mus, F., Gutknecht, A.E., Martinez, H.A., Tripet, B.P., Lange, B.M. et al. (2018) Coenzyme M biosynthesis in bacteria involves phosphate elimination by a functionally distinct member of the aspartase/fumarase superfamily. *The Journal of Biological Chemistry*, 293, 5236–5246.

Reed, B., Blazeck, J. & Alper, H. (2012) Evolution of an alkane-inducible biosensor for increased responsiveness to short-chain alkanes. *Journal of Biotechnology*, 158, 75–79.

Rogers, J.K., Guzman, C.D., Taylor, N.D., Raman, S., Anderson, K. & Church, G.M. (2015) Synthetic biosensors for precise gene control and real-time monitoring of metabolites. *Nucleic Acids Research*, 43, 7648–7660.

Russell, A.D. (1990) Bacterial spores and chemical sporicidal agents. *Clinical Microbiology Reviews*, 3, 99–119.

Sambrook, J., Fritsch, E.R. & Maniatis, T. (1989) *Molecular cloning: a laboratory manual*, 2nd edition. NY: Cold Spring Harbor Laboratory Press.

Santala, S., Karp, M. & Santala, V. (2012) Monitoring alkane degradation by single BioBrick integration to an optimal cellular framework. *ACS Synthetic Biology*, 1, 60–64.

Sevilla, E., Yuste, L., Moreno, R. & Rojo, F. (2017) Differential expression of the three *Alcanivorax borkumensis* SK2 genes coding for the P450 cytochromes involved in the assimilation of hydrocarbons. *Environmental Microbiology Reports*, 9, 797–808.

Sevilla, E., Yuste, L. & Rojo, F. (2015) Marine hydrocarbonoclastic bacteria as whole-cell biosensors for n -alkanes. *Microbial Biotechnology*, 8, 693–706.

Shennan, J.L. (2006) Utilisation of C2-C4 gaseous hydrocarbons and isoprene by microorganisms. *Journal of Chemical Technology and Biotechnology*, 81, 237–256.

Snapper, S.B., Melton, R.E., Mustafa, S., Kieser, T. & Jacobs, W.R. (1990) Isolation and characterization of efficient plasmid transformation mutants of *mycobacterium smegmatis*. *Molecular Microbiology*, 4, 1911–1919.

Stekel, D.J. & Jenkins, D.J. (2008) Strong negative self regulation of prokaryotic transcription factors increases the intrinsic noise of protein expression. *BMC Systems Biology*, 2, 6.

Sticher, P., Jaspers, M.C.M., Stemmler, K., Harms, H., Zehnder, A.J.B. & Van der Meer, J.R. (1997) Development and characterization of a whole-cell bioluminescent sensor for bioavailable middle-chain alkanes in contaminated groundwater samples. *Applied and Environmental Microbiology*, 63, 4053–4060.

Tellechea-Luzardo, J., Stiebritz, M.T. & Carbonell, P. (2023) Transcription factor-based biosensors for screening and dynamic regulation. *Frontiers in Bioengineering and Biotechnology*, 11, 1118702.

Triccas, J.A., Parish, T., Britton, W.J. & Gicquel, B. (1998) An inducible expression system permitting the efficient purification of a recombinant antigen from *mycobacterium smegmatis*. *FEMS Microbiology Letters*, 167, 151–156.

United Nations Environment Programme. (2021) Food Waste Index Report. https://www.unep.org/resources/report/unep-food-waste-index-report-2021

Vaidya, A.M. & Annapure, U.S. (2019) *Enzymes in biosensors for food quality assessment. Chapter 38 in enzymes in food biotechnology: production, applications, and future prospects*. Cambridge, MA, USA: Academic Press.

Van Beilen, J.B., Panke, S., Lucchini, S., Franchini, A.G., Rothlisberger, M. & Witholt, B. (2001) Analysis of *pseudomonas putida* alkane-degradation gene clusters and flanking insertion sequences: evolution and regulation of the *alk* genes. *Microbiology*, 147, 1621–1630.

Willardson, B.M., Wilkins, J.F., Rand, T.A., Schupp, J.M., Hill, K.K., Keim, P. et al. (1998) Development and testing of a bacterial biosensor for toluene-based environmental contaminants. *Applied and Environmental Microbiology*, 64, 1006–1012.

Wu, W., Zhang, L., Yao, L., Tan, X., Liu, X. & Lu, X. (2015) Genetically assembled fluorescent biosensor for in situ detection of biosynthesized alkanes. *Scientific Reports*, 5, 10907.

Yacovitch, T.I., Dyroff, C., Roscioli, J.R., Daube, C., Mcmanus, J.B. & Herndon, S.C. (2022) Ethylene oxide monitor with part-per-trillion precision for *in-situ* measurements. *Atmospheric Measurement Techniques*, 16, 1915–1921.

Zhang, D., Fakhrullin, R.F., Özmen, M., Wang, H., Wang, J., Paunov, V.N. et al. (2011) Functionalization of whole-cell bacterial reporters with magnetic nanoparticles. *Microbial Biotechnology*, 4, 89–97.

Zhang, D., He, Y., Wang, Y., Wang, H., Wu, L., Aries, E. et al. (2012) Whole-cell bacterial bioreporter for actively searching and sensing of alkanes and oil spills. *Microbial Biotechnology*, 5, 87–97.

SUPPORTING INFORMATION

Additional supporting information can be found online in the Supporting Information section at the end of this article.

How to cite this article: Moratti, C.F., Yang, S.N.N., Scott, C. & Coleman, N.V. (2024) Development of a whole-cell biosensor for ethylene oxide and ethylene. *Microbial Biotechnology*, 17, e14511. Available from: https://doi.org/10.1111/1751-7915.14511